GEORGIA INSTITUTE OF TECHNOLOGY — OFFICE OF CONTRACT ADMINISTRATION

PROJECT ADMINISTRATION DATA SHEET

[x] ORIGINAL [ ] REVISION NO. ____

Project No. E-19-666 GTRI/~~GTE~~ DATE 5 / 24 / 84

Project Director: Dr. A. P. Yoganathan GA School/~~Dept~~ ChE

Sponsor: American Heart Association; Georgia Affiliate, Inc., Atlanta, GA

Type Agreement: Grant-in-Aid Agreement (no number)

Award Period: From 7/1/84 To 6/30/85 (Performance) 8/30/85 (Reports)

Sponsor Amount:	This Change	Total to Date
Estimated:	$	$ 16,500
Funded:	$	$ 16,500

Cost Sharing Amount: $ ____ Cost Sharing No: ____

Title: "Computer Simulation of Flow Through Trileaflet Heart Valves"

ADMINISTRATIVE DATA — OCA Contact Lynn Boyd x4820

1) Sponsor Technical Contact:

Spencer King III, M.D., President
American Heart Association
Georgia Affiliate
2581 Piedmont Rd., NE
P.O. Box 13589
Atlanta, GA 30324 (404) 261-2260

2) Sponsor Admin/Contractual Matters:

Leisle A. Ewing
Assistant Program Director
2581 Piedmont Road, NE
P. O. Box 13589
Atlanta, GA 30324
(404) 261-2260

Defense Priority Rating: n/a Military Security Classification: n/a

(or) Company/Industrial Proprietary: n/a

RESTRICTIONS

See Attached n/a Supplemental Information Sheet for Additional Requirements.

Travel: Foreign travel must have prior approval – Contact OCA in each case. Domestic travel requires sponsor approval where total will exceed greater of $500 or 125% of approved proposal budget category.

Equipment: Title vests with GIT.

COMMENTS:

Sponsor I.D. #02.500.000.84.009

COPIES TO:

Project Director
Research Administrative Network
Research Property Management
Accounting
Procurement/EES Supply Services
Research Security Services
Reports Coordinator (OCA)
Research Communications (2)
GTRI
Library
Project File
Other Newton

FORM OCA 4 383

GEORGIA INSTITUTE OF TECHNOLOGY OFFICE OF CONTRACT ADMINISTRATION

SPONSORED PROJECT TERMINATION/CLOSEOUT SHEET

Date 7/22/85

Project No. E-19-669 6 School/Lab XXX ChE

Includes Subproject No.(s) None Indicated

Project Director(s) Dr. A. P. Yoganathan GTRC / GCX

Sponsor American Heart Association Georgia Affiliate

Title Computer Simulation of Flow Through Trileaflet Heart Valves

Effective Completion Date: 6/30/85 (Performance) 7/1/85 (Reports)

Grant/Contract Closeout Actions Remaining:

- [ ] None
- [X] Final Invoice or Final Fiscal Report
- [ ] Closing Documents
- [ ] Final Report of Inventions
- [ ] Govt. Property Inventory & Related Certificate
- [ ] Classified Material Certificate
- [ ] Other

Continues Project No. N/A Continued by Project No. E-19-636

COPIES TO:

Project Director
Research Administrative Network
Research Property Management
Accounting
Procurement/GTRI Supply Services
Research Security Services
Reports Coordinator (OCA)
Legal Services
Library
GTRC
Research Communications (2)
Project File SB 7/23
Other A. Jones; M. Heyser

FORM OCA 69 285

GEORGIA TECH 1885-1985

DESIGNING TOMORROW TODAY

Georgia Institute of Technology
School of Chemical Engineering
Atlanta, Georgia 30332-0100
(404) 894-

June 26, 1985

Mr. Charles Taylor
American Heart Association -
Georgia Affiliate
2581 Piedmont Road N.E.
P.O. Box 13589
Atlanta, GA 30324

Dear Mr. Taylor:

Enclosed are three copies of my final report on my research grant, for the period 7/1/84 - 6/30/85. If you need any further information, please let me know.

Sincerely,

Ajit P. Yoganathan
Associate Professor
Chairman, Bioengineering Committee

APY:psh
Enclosures

cc: Dr. G. W. Poehlein
Mr. John Shonk - OCA

AMERICAN HEART ASSOCIATION - GEORGIA AFFILIATE

COMPUTER SIMULATION OF FLOW THROUGH TRILEAFLET HEART VALVES

(GRANT-IN-AID)

FINAL REPORT (7/1/84 - 6/30/85)

I. Principal Investigator

Professor Ajit P. Yoganathan, Ph.D., Georgia Tech

II. Project Report

(A) General

Both in vivo and in vitro hemodynamic studies indicate that the trileaflet tissue valves in current clinical use have inferior fluid dynamic characteristics, especially in the smaller sizes. The perceived increased use of the new low-pressure fixed tissue valves for heart valve replacement and in valved conduits, together with the need for cheap, disposable and fluid mechanically efficient trileaflet valves in short and long term LVADs require detailed fundamental studies of the trileaflet design concept. In vitro studies indicate that the fluid dynamic characteristics of some of the current trileaflet designs can be improved by improving the design characteristics of the valve leaflets and supporting stent structures.

(B) Computational Scheme and Methodology

The aim of the present study is to provide a relatively realistic simulation of steady Newtonian blood flow through trileaflet tissue valves of varying degrees of stenosis. The ultimate goal of this research effort is to develop the means for designing trileaflet valves which are more fluid dynamically efficient and clinically useful. The aortic trileaflet tissue valve design was chosen as the subject of this study, since it is the only popular valve in current clinical use which is approximately axisymmetric. An axisymmetric geometry is computationally more convenient since it involves only two dimensional equations. An extension to three dimensions may be conceptually simple but the actual implementation is very difficult. The geometry and dimensions of the aorta were designed from angiographic studies and measurements made from cadavers. The valve dimensions were obtained from tissue leaflet photography studies conducted on tissue bioprostheses of varying degrees of stenosis. The non-rectangular nature of this valve necessitated the use of a body conforming grid. Thompson's method coupled with a Chimera grid system was chosen for this purpose. The Chimera grid was used to avoid a grid with highly skewed cells. Turbulence was simulated using the k-ε model with the wall function method. This decision was made after comparing the k-ε model's performance with that of lower order models, and after considering the increased computer time requirements and decreased stability of more complex models, such as the Reynolds stress model.

(C) Geometries and Simulations Studied

The dimensions of the aortic geometry used in this study is similar to the aortic flow chamber used in our experimental work with some slight modifications. The internal diameter of the inlet and outlet tubes is 25.4 mm. The axisymmetric sinus is 31.5 mm in diameter and 29.2 mm in length. The thick leaflet was necessary to avoid a highly skewed grid near the leaflet tip.

Table 1 is a list of all the geometries and simulations which were investigated. No coordinate attraction was used in preparing grid 1 for each geometry. However, coordinate attraction was used for grid 2 in order to fill the region between the leaflet tip and the end of the sinus with enough computational nodes. Otherwise the lines were too concentrated around the leaflet and too sparse elsewhere which led to an unstable computation. Figures 1 through 5 present the grids which were used for each model. Figure 6A shows aortic model A2 when rotated about the centerline. Figure 6B shows the three dimensional projection of model A2 and labels various portions of the model. The fluid used in all simulations was a Newtonian fluid of viscosity and specific gravity equal to that of blood, which are 3.0 centipoise and 1.07, respectively. The flow rate through the aortic models in all turbulent simulations was 30 liter/min, corresponding to a typical peak systolic flow rate across the aortic valve of an average person at rest. The dimensions of the valve leaflet flow areas were chosen to cover the wide range of effective flow areas observed with trileaflet valves in current clinical use. For example, a size 27mm Hancock

porcine tissue valve has an effective flow area of about 1.7 cm^2, a size 27mm Ionescu-Shiley pericardial tissue valve has an effective flow area of about 2.4 cm^2 (Yoganathan, 1983), and an undiseased natural aortic valve has a flow area of approximately 5.0 cm^3. The results of the computer simulation are given in the following sections.

(D) Streamline Plots

Figures 7a and 7b are streamline plots for models A2 and A5. Only the portion of each flow field which is of interest is presented. Since the region behind the valve leaflet contains very low velocities, no streamlines are shown in this region. These plots illustrate the effects of increasing valve stenosis. Models A4 and A5 disturb the flow field only to a small extent, and cause relatively small recirculation regions to be produced, which are contained within the sinus region (1.1 diameters long). The maximum width of the recirculation regions are 4 mm for model A4, and 2 mm for A5. Model A3 produces a larger recirculation zone which escapes the sinus region, and reattaches further downstream (1.4 diameters). The maximum width of this region is 6 mm. Model A2 reattaches even further downstream (1.7 diameters), with a maximum width of 7 mm. Model A1 is so severely stenotic, that sufficient computer memory to extend the tube far enough downstream for reattachment to occur did not exist.

(E) Velocity Profiles

Velocity profiles are presented in this section at various locations in each of the five models. The velocities have been non-dimensionalized by a bulk velocity at 100 cm/sec. The radial and axial distances are non-dimensionalized by the diameter of the tube leading into the test chamber (2.54 cm). All upstream and downstream distances are measured from the valve seat. Beginning with model A1, (Figure 8), the velocity profile at 0.1 diameters upstream (just as the fluid begins to enter the valve) shows that the flow is accelerated near the center, with a maximum non-dimensionalized value approaching 2.2. The velocity gradient near the wall has decreased accordingly. The profile across the valve itself exhibits an off-center peak with a non-dimensionalized velocity of 5.3. This is due to the rapid acceleration which has taken place near the wall, compared to the acceleration near the center. A profile further downstream, at 0.65 diameters, indicates the very low velocities which exist in the stagnant region near the wall. The central jet which is observed in the streamline plot for model A1 is evident in the velocitiy profile at this region. In addition, the velocity gradient increases dramatically adjacent to the stagnant region. The velocity field exhibits a very small positive wall gradient, indicating a low velocity clockwise rotating recirculation bubble. Further downstream, at 1.67 diameters, recirculation is evident in the large negative velocities near the wall.

Model A2 is considered next in figure 9. The velocity profile made 0.1 diameters upstream of the valve shows the decreased wall gradient and accelerated core. After the flow has entered the valve, an off-center peak is observed, with a maximum value of 3.2. The profile at 0.55 diameters exhibits a positive wall gradient, with a central jet, and correspondingly high velocity gradients. This positive wall gradient is a result of the clockwise rotating recirculation bubble which extends behind the valve leaflet. The profile taken at 0.85 diameters indicates a large recirculation region near the wall. 1.0 diameters downstream, this region has narrowed in width, but maintained high negative velocities with a non-dimensionalized value of -0.4. Further downstream, at 1.5 diameters, the recirculation region persists, until it has reattached at about 1.7 diameters. At this point, the profile has developed an off-center peak. This peak is thought to be due to acceleration of the fluid near the wall from the sudden change in the wall shape, corresponding to the end of the sinus region. After reattachment, the simulated flow recovers quickly to become fully developed. This is due to the limit on computer memory, which did not allow sufficient tube length downstream of the valve to allow the simulated flow field to become fully developed on its own before imposing the fully developed boundary condition.

In model A3, (Figure 10), the valve constriction decreases, with less disturbance to the flow field. The profile made 0.1 diameters upstream of the valve exhibits the centerline acceleration of the fluid. Inside the valve, an off-center peak

is again observed, with a maxmimum non-dimensionalized value of 2.0. The profile made at 0.5 diameters shows the positive wall gradient indicative of a clockwise rotating recirculation bubble. In addition, the central jet is evident in this profile. At 0.8 diameters the negative velocities near the wall increase to a non-dimensionalized velocity of -0.1. The center jet already exhibits an off-center velocity maximum. This peak is thought to be due to the sudden change in wall shape at the end of the sinus region. At 1.0 diameter this off-center maximum persists. The flow has reattached and is beginning to recover at 1.5 diameters.

In model A4, (Figure 11), the flow is less disturbed than in model A3. The profile was taken just upstream of the valve, and shows that the flow has not deviated significantly from a fully developed profile. Inside the valve the off-center peak is not observed, although the flow has accelerated to a maximum non-dimensionalized velocity of 1.6. The profile taken at 0.6 diameters, as the fluid exits the valve shows the positive wall gradient, indicative of a clockwise recirculation region. At 0.9 diameters a small recirculation region exists near the wall, but has reattached at the end of the sinus region, 1.14 diameters downstream. The profile is nearly fully developed turbulent, a short distance further downstream.

Finally, model A5, (Figure 12), which approximates the natural aortic valve, disturbs the flow the least. The profile, taken 0.1 diameters upstream of the valve, shows that the flow field does not deviate significantly from the fully developed

profile. The same is true inside the valve. As the fluid exits, it again sets up a clockwise rotating recirculation extending behind the valve leaflet. At 0.9 diameters the velocities near the wall remain negative. The recirculation is again contained inside the sinus region, with the flow reattaching at about 1.14 diameters downstream.

The effects of increasing valve stenosis are evident as one studies the velocity profiles from models A1 through A5. At the upstream location, as the fluid enters the valve, the peak velocity increases from 1.2 in model A5 to 2.2 in model A1. The profiles taken inside the valve exhibit higher velocities in the more stenosed valves due to the smaller flow area, but also show an off-center maximum for models A1, A2, and A3. This is due to the rapid fluid acceleration near the wall, and does not persist after the fluid has exited the valve. After exiting the valve, all five models set up a clockwise rotating recirculation which extends behind the valve leaflet, and is evident in the positive velocities near the wall at the point where the fluid exits the valve.

(F) Turbulent Shear Stress

Figures 13 through 18 are examples of the turbulent shear stresses profiles obtained with models A1, A2, A3, A4 and A5. Beginning with model A1, (Figure 13), the profiles exhibit elevated shear stresses upstream of the valve, exceeding 80 N/m^2. This is due to the acceleration of the fluid in the core. As the fluid enters the valve, a high velocity gradient

exists near the wall, increasing shear stress values to 350 N/m^2 near the leaflet wall. As the fluid progresses downstream it exits the valve as a jet bounded by a stagnant region. Here the turbulent shear stress increases to about 520 N/m^2.

In model A2 (Figure 14), the shear stresses upstream of the valve remain relatively low (30 N/m^2), since the core is not accelerated to the extent seen in model A1. The shear stress increases to 150 N/m^2 near the inside wall of the valve, due to the high velocity gradient at this location. The region of increased shear stresses continues downstream as the fluid exits the valve, producing a jet bounded by an annular recirculation region. The velocity gradients increase due to the effects of the recirculation, and consequently increase the shear stress values to a maximum of 310 N/m^2. The peak shear stress is followed by a rapid decrease to 30 N/m^2 before the recirculation region reattaches.

Flow through model A3 (Figure 15) experiences less turbulent shear stress than in A2. Upstream of the valve, the shear stresses remain below 25 N/m^2, since the fluid core does not experience much acceleration. As the fluid flows through the valve, the wall velocity gradient increases, resulting in the shear stress increasing to 80 N/m^2 near the wall. After the fluid exits the valve, the velocity gradients increase still more, and the shear stresses increase to about 125 N/m^2 near the recirculation region. The values in the model then quickly decay to 50-60 N/m^2 as the velocities in the recirculation region begin to slow down.

Model A4 also produces elevated turbulent shear stresses (Figure 16). The stresses remain low upstream of the valve, since the core acceleration is very small, and increase inside the valve to 70 N/m^2 near the wall. After the fluid exits the valve, the shear stresses increase to about 150 N/m^2 at 0.9 diameters, as a direct result of the increased velocity gradients near the recirculation region. The shear stresses then rapidly decay back down to 25 N/m^2.

Finally, the less stenotic valve of model A5 produces slightly elevated Reynolds stresses (Figure 17). Upstream of the valve, and also inside the valve, the shear stress remains low, and increases to only 25 N/m^2 inside the valve, since the velocity gradients increase only slightly. After the fluid exits the valve, the peak shear stress decays rapidly from 50 to 25 N/m^2.

Since the production of turbulence is due to velocity gradients in the flow, it is possible to correlate velocity gradients with turbulent shear stresses. This is indeed the case, as the regions of highest velocity gradient and fluid acceleration correspond with the locations of highest turbulent shear stress. Peak values for turbulent shear stresses ranged from 50 to 520 N/m^2 downstream of the valves. These values are high enough to cause sublethal and/or lethal damage to both platelets and red blood cells in the fluid flowing through the valve. Furthermore, the turbulent shear stresses within the valves increase dramatically with increasing stenosis. The peak shear stresses inside the valves were 350, 150, 80, 70, and 25

N/m^2 for models A1 through A5, respectively. Clearly, the effects of decreasing stenosis can be seen.

(G) Pressure Drops

Table 2 lists the pressure drops observed with the various aortic valve models. Model A1 exhibits the highest pressure drop across the valve, becoming as high as 375 mm Hg inside the valve. The pressure difference then recovers to 250 mm Hg. The pressure drop in model A1 remains high, since the central jet is not allowed to reattach and recover due to the lack of computer memory to extend the grid far enough downstream. Model A2 indicates a substantial improvement in pressure drop for a small change in valve constriction. The peak pressure drop inside the valve is 125 mm Hg. The pressure recovers quickly, to produce a pressure difference of 20 mm Hg at 1.6 diameters. In model A3 the flow is accelerated less than in model A2, such that the pressure drop in the valve is correspondingly lower. The peak pressure difference again occurs inside the valve at 40 mm Hg. The pressure recovers quickly, to give a pressure drop of 9 mm Hg at 1.6 diameters downstream. Model A4 exhibits a lower pressure difference of 7 mm Hg inside the valve, and recovers to a pressure drop of less than 1 mm Hg at 1.6 diameters . Finally, model A5 exhibits a very low pressure drop of less than 1 mm Hg inside the valve, going to complete recovery downstream of the valve.

(H) Lay Summary

This research work is mainly directed towards understanding the flow of blood through various designs of trileaflet heart valve prostheses. It is proposed to use a sophisticated computer model to evaluate how various parameters of trileaflet valve designs affect their performance. Such parameters are: (i) leaflet shape, (ii) leaflet size, (iii) stent design and (iv) orifice design. These parameters will be varied in the computer model in order to optimize the designs of trileaflet valves.

Trileaflet valves in current clinical use do not possess good hemodynamic (fluid mechanic) characteristics, especially in the smaller sizes. It is our opinion these poor performance characteristics are due to poor design criteria. With the proposed computer model it is planned to study a variety of trileaflet valve designs which could be used: (i) for heart valve replacement, (ii) in short and long term left ventricular assist devices, (iii) in a total artificial heart.

III. Collaborators

The following graduate students at Georgia Tech worked on the project:

Dana Stevenson - Ph.D. Student

Frank P. Williams - Ph.D. Student

IV. Publications

(A) Abstracts and Presentations

1. Stevenson, D. M. and Yoganathan, A. P., "Computer simulation of steady turbulent flow through trileaflet heart valves," Proceedings of the Joint ASME/ASCE Mechanics Conference, Albuquerque, NM, June 1985.

(B) Manuscripts

1. Stevenson, D. M. and Yoganathan, A. P., "Numerical simulation of steady turbulent flow through trileaflet aortic heart valves, Part I: Computational scheme and methodology," submitted to Journal of Biomechanics.

2. Stevenson, D. M., Yoganathan, A. P. and Williams, F. P., "Part II: Results on five models," submitted to Journal of Biomechanics.

Table 1
List of All Geometries and Simulations Studied

Geometry	Entrance Diameter (cm)	Valve+ Leaflet Flow Area (cm^2)	Laminar or Turbulent	Reynolds Number
Straight tube	2.54	-	Laminar	1,500
Straight tube	2.54	-	Turbulent	15,000
Stenosis model M0	2.54	1.27*	Laminar	50
Stenosis model M4	2.54	1.27*	Turbulent	15,000
Aortic model A1	2.54	1.1	Turbulent	9,000
Aortic model A2	2.54	1.6	Laminar	50
Aortic model A2	2.54	1.6	Turbulent	9,000
Aortic model A3	2.54	2.5	Turbulent	9,000
Aortic model A4	2.54	3.5	Turbulent	9,000
Aortic model A5	2.54	5.0	Turbulent	9,000

* Stenosis throat area.

+ See Figure 6b.

Table 2

Pressure Differences at Three Locations

in All Five Models

	β*	ΔP (Inside Valve) (mm Hg)	ΔP (1.0 diameter downstream) (mm Hg)	ΔP (1.6 diameter downstream) (mm Hg)
Model A1	0.22	375	220	230
Model A2	0.32	125	38	20
Model A3	0.49	40	15	9
Model A4	0.69	7	3	0
Model A5	0.99	1	0	0

* Ratio of valve orifice area to flow area upstream of the valve.

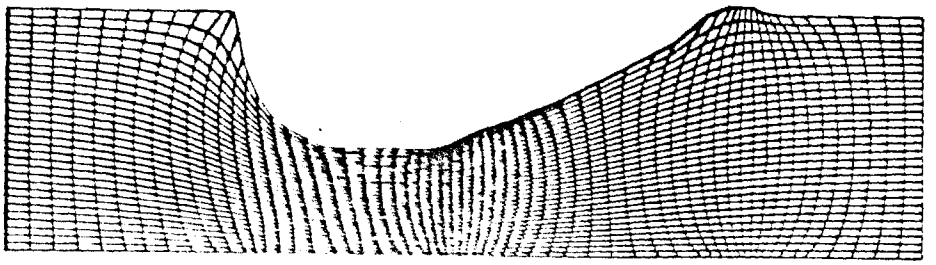

grid 1

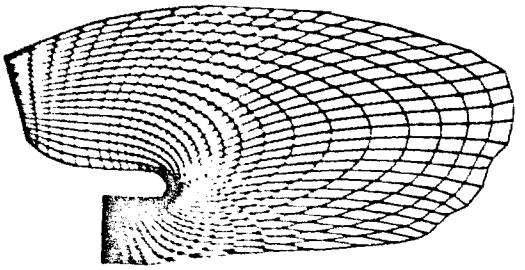

grid 2

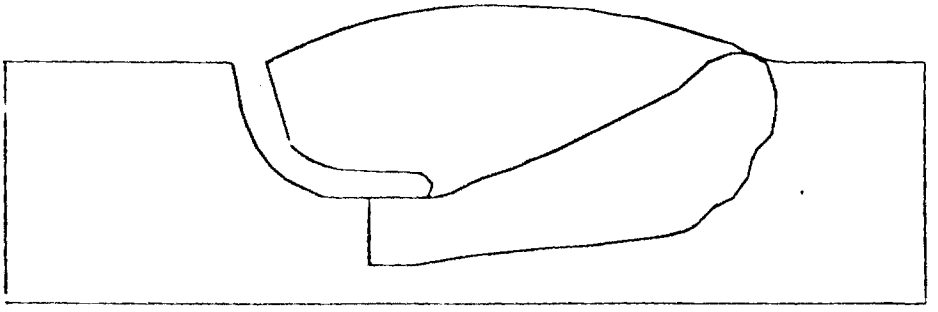

both grids overlapped

Figure 1. Grids for aortic valve model A1

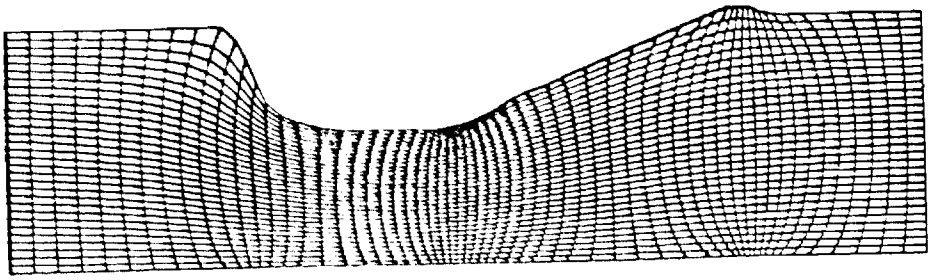

grid 1

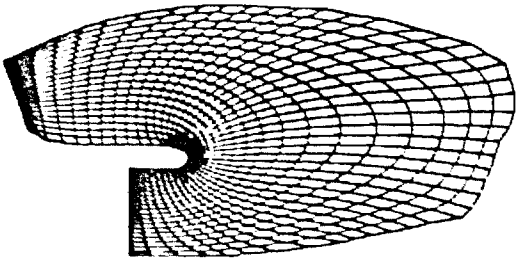

grid2

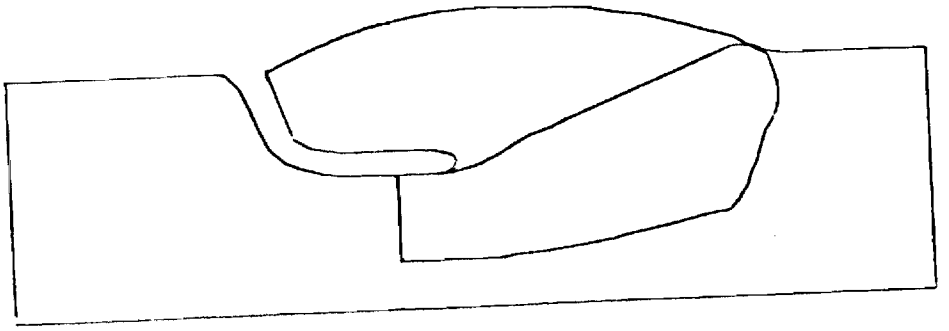

both grids overlapped

Figure 2. Grids for aortic valve model A2

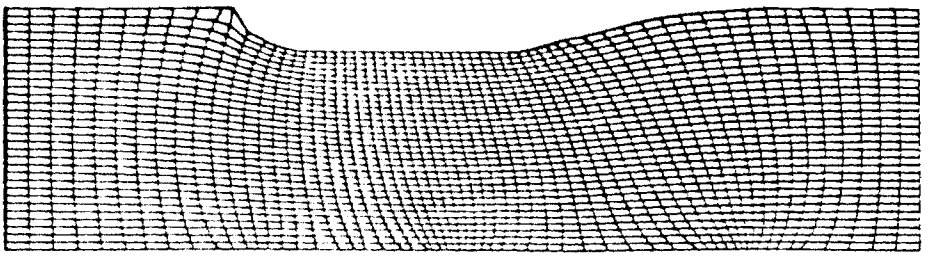

grid 1

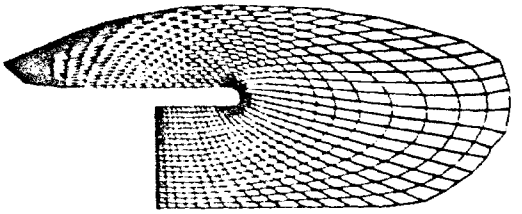

grid 2

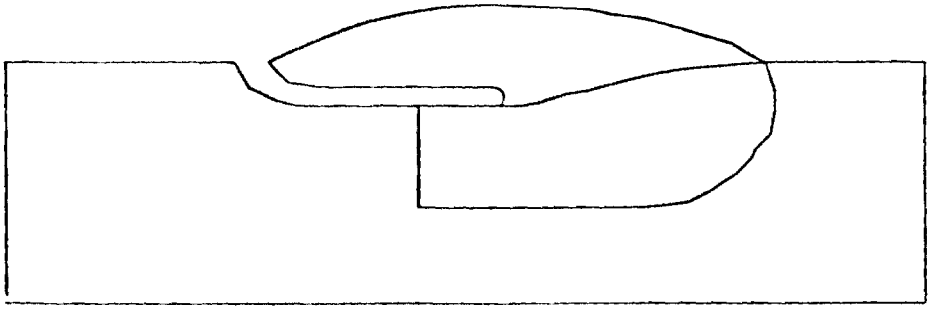

both grids overlapped

Figure 4. Grids for aortic valve model A4

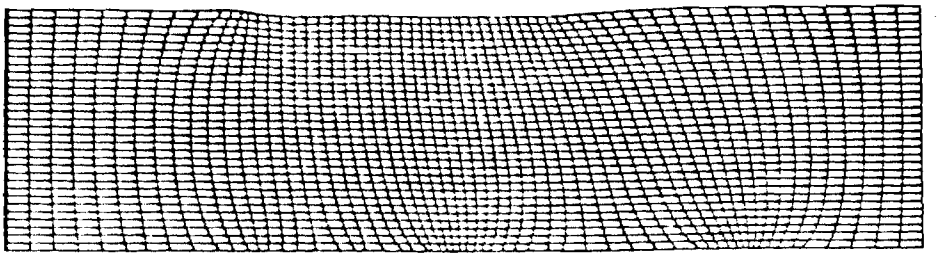

grid 1

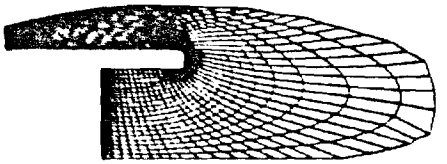

grid 2

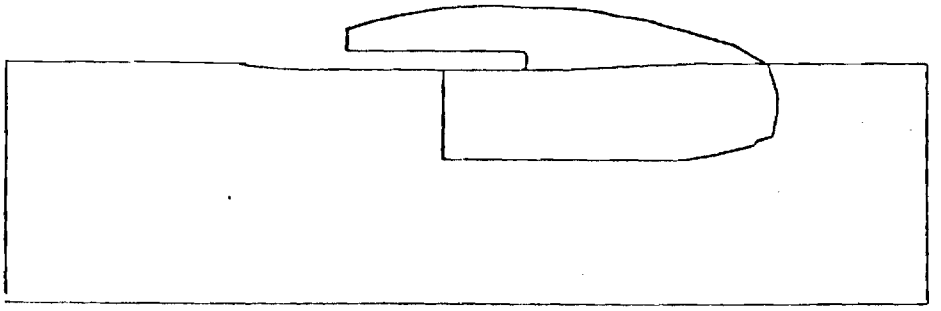

both grids overlapped

Figure 5. Grids for aortic valve model A5

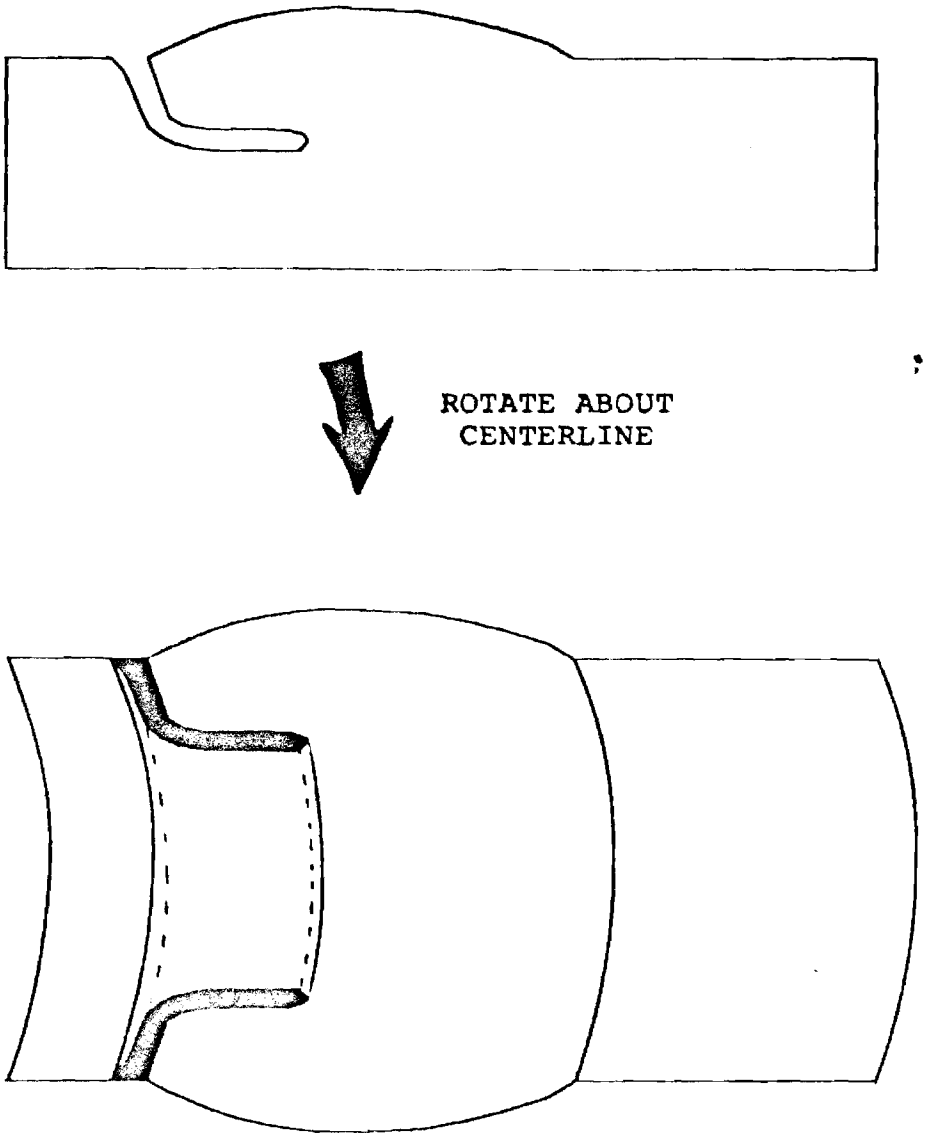

Figure 6a. Schematic of aortic model A2 rotated about the centerline

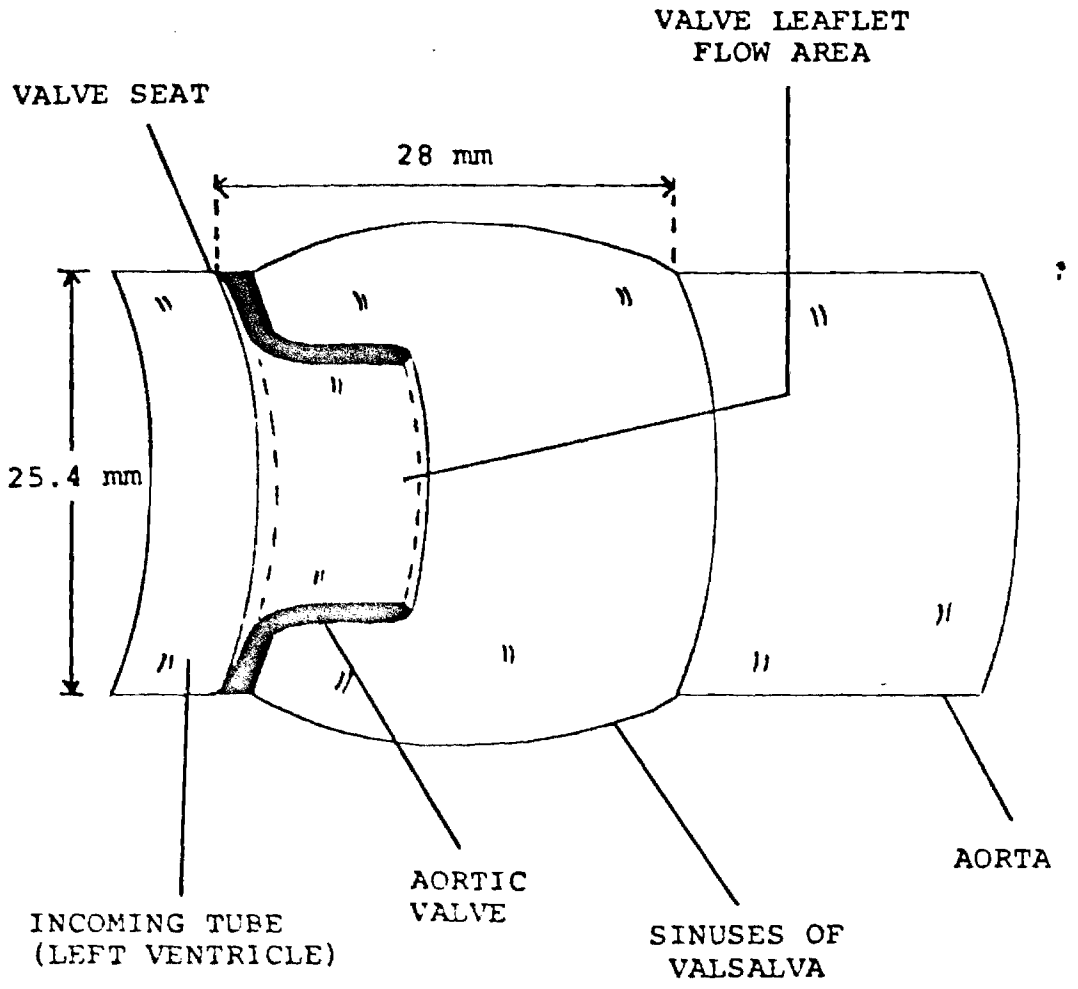

Figure 6b. Schematic of the three dimensional projection of the trileaflet valve geometry

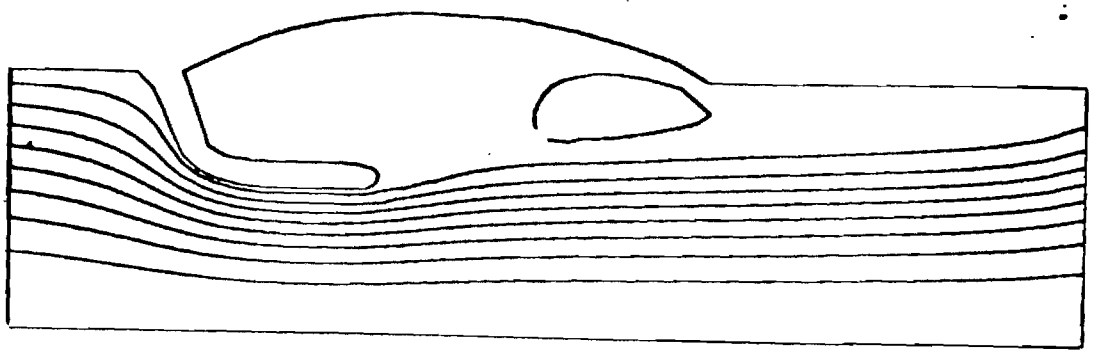

Figure 7a: Streamline Plot for Model A2

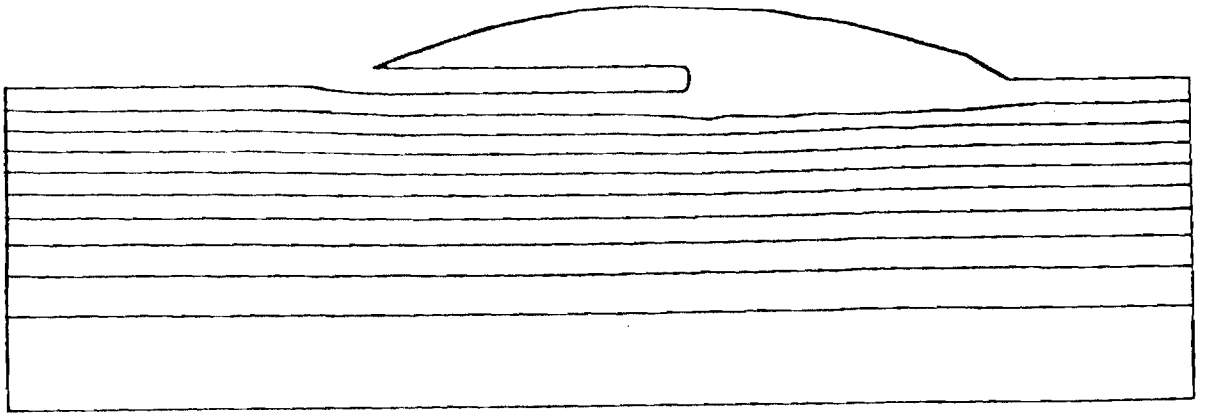

Figure 7b: Streamline Plot for Model A5

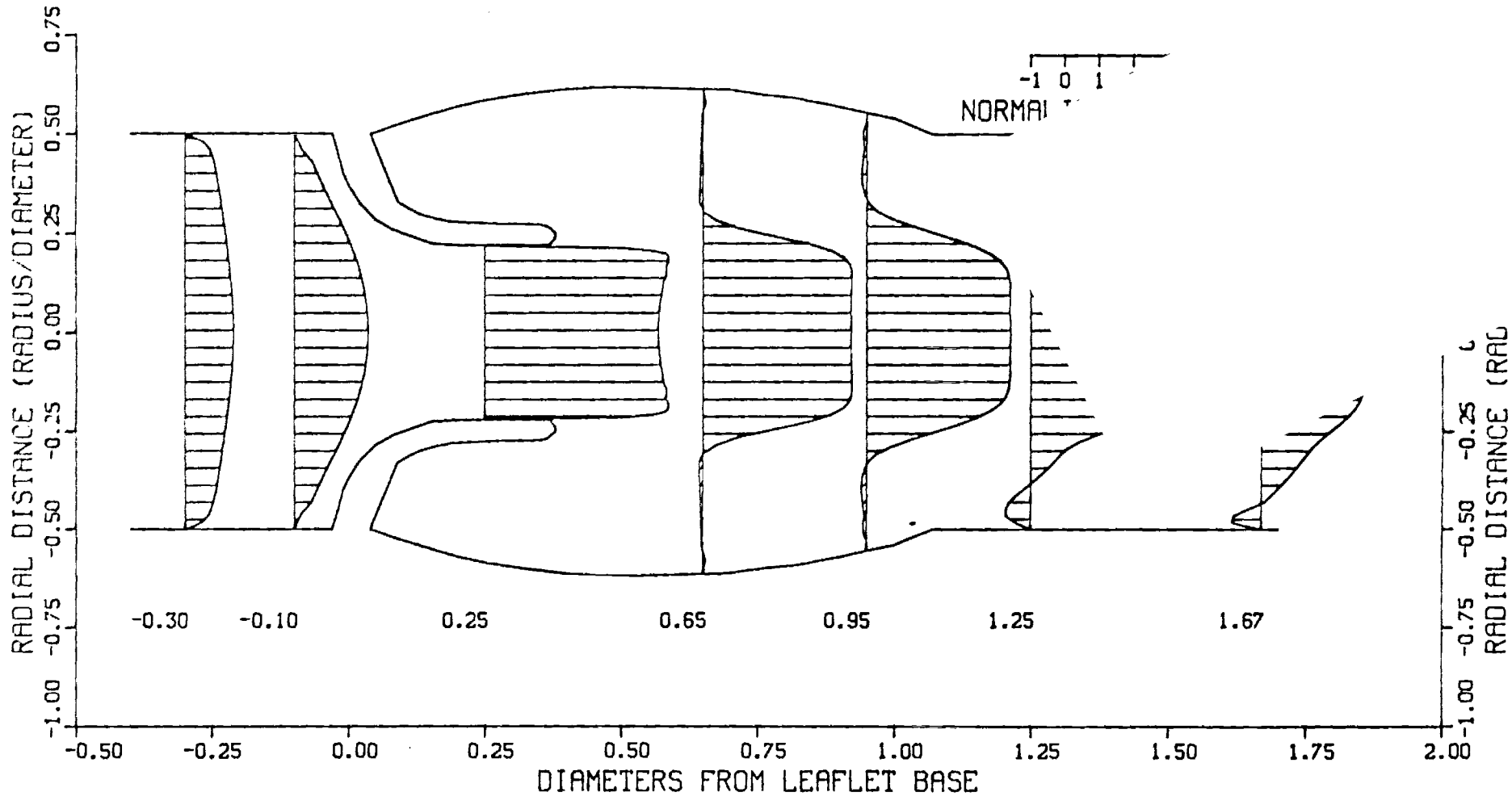

Figure 8: Velocity Profiles at Various Locations in Model A1

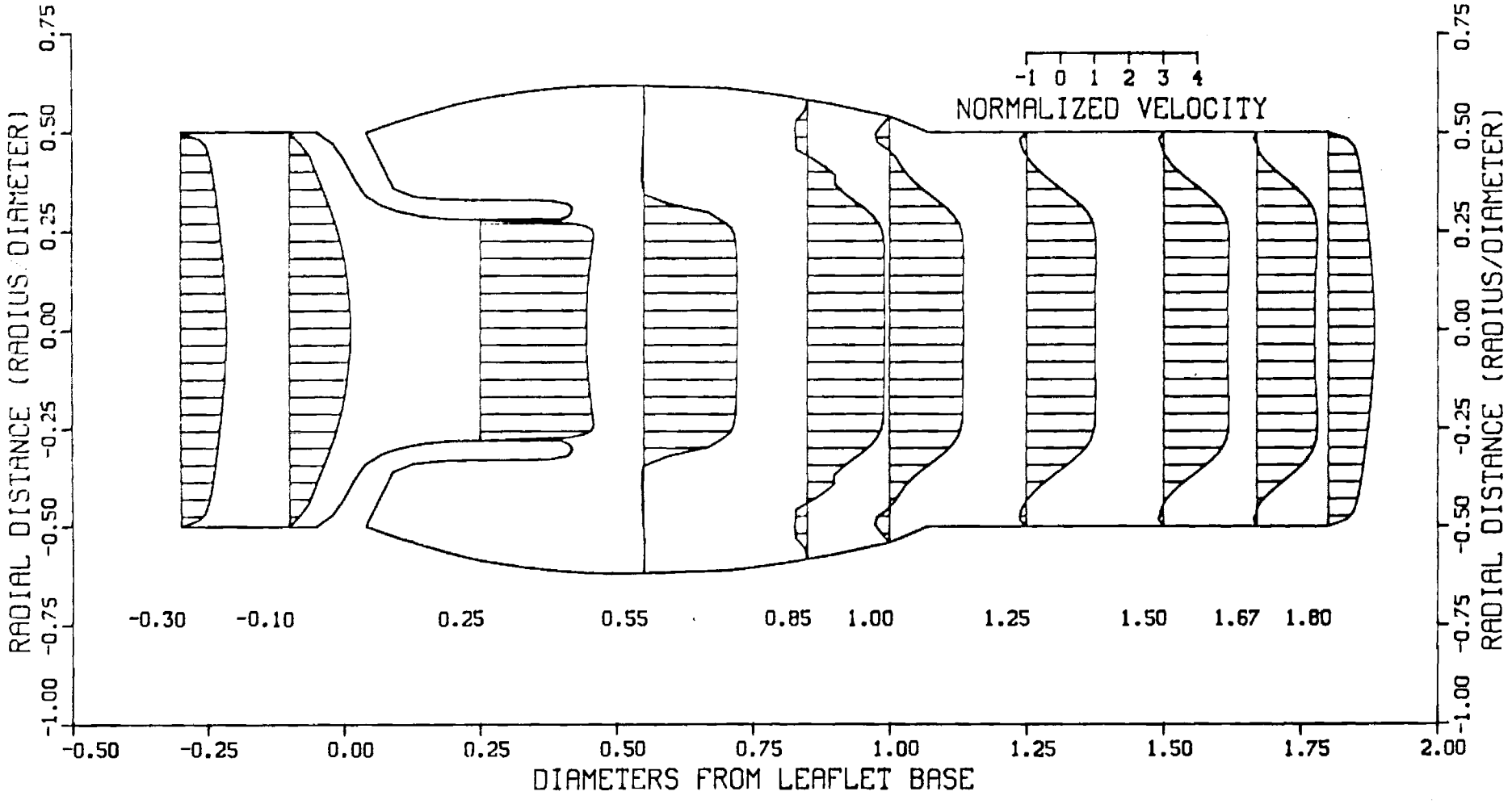

Figure 9: Velocity Profiles at Various Locations in Model A2

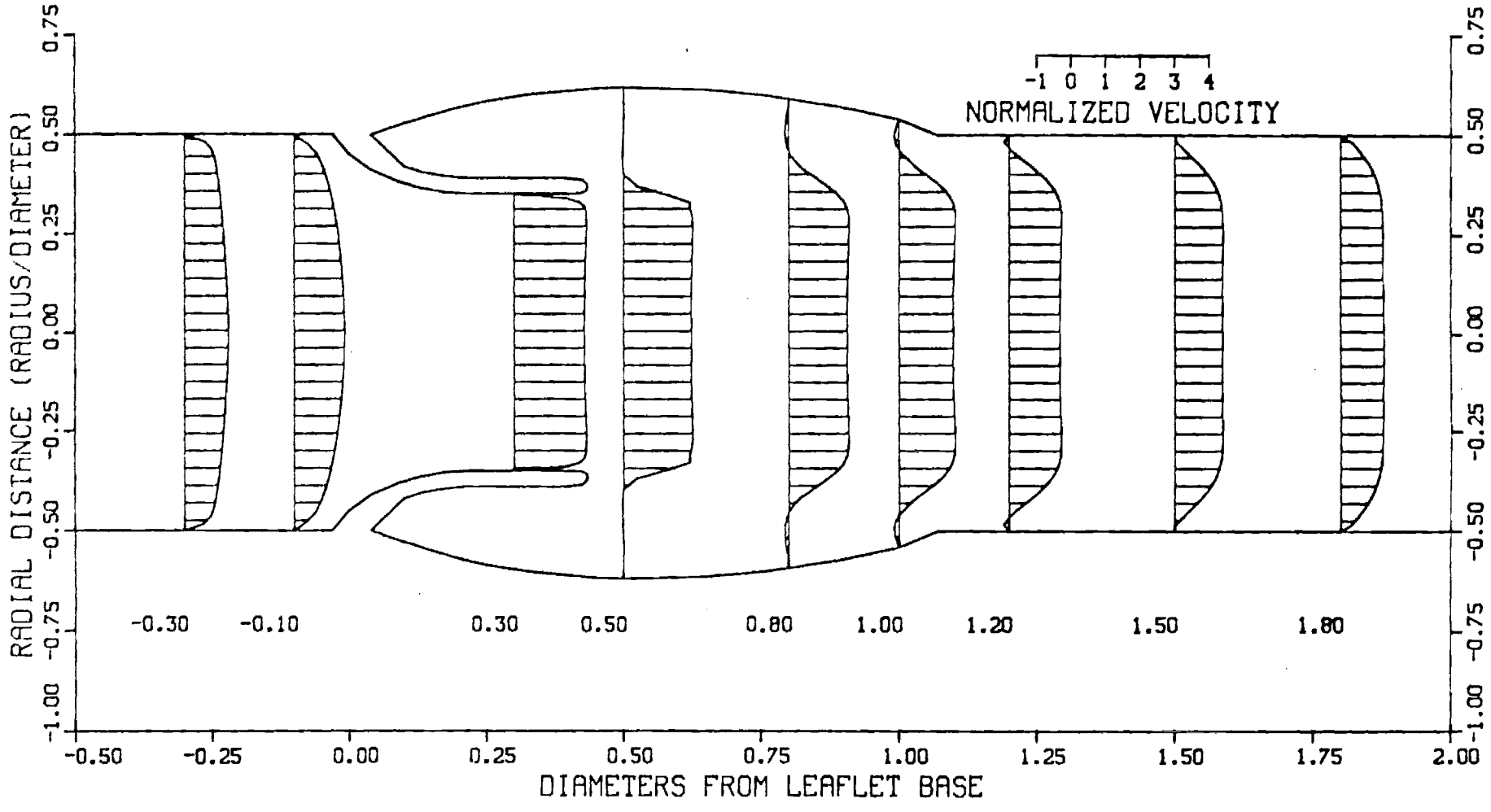

Figure 10: Velocity Profiles at Various Locations in Model A3

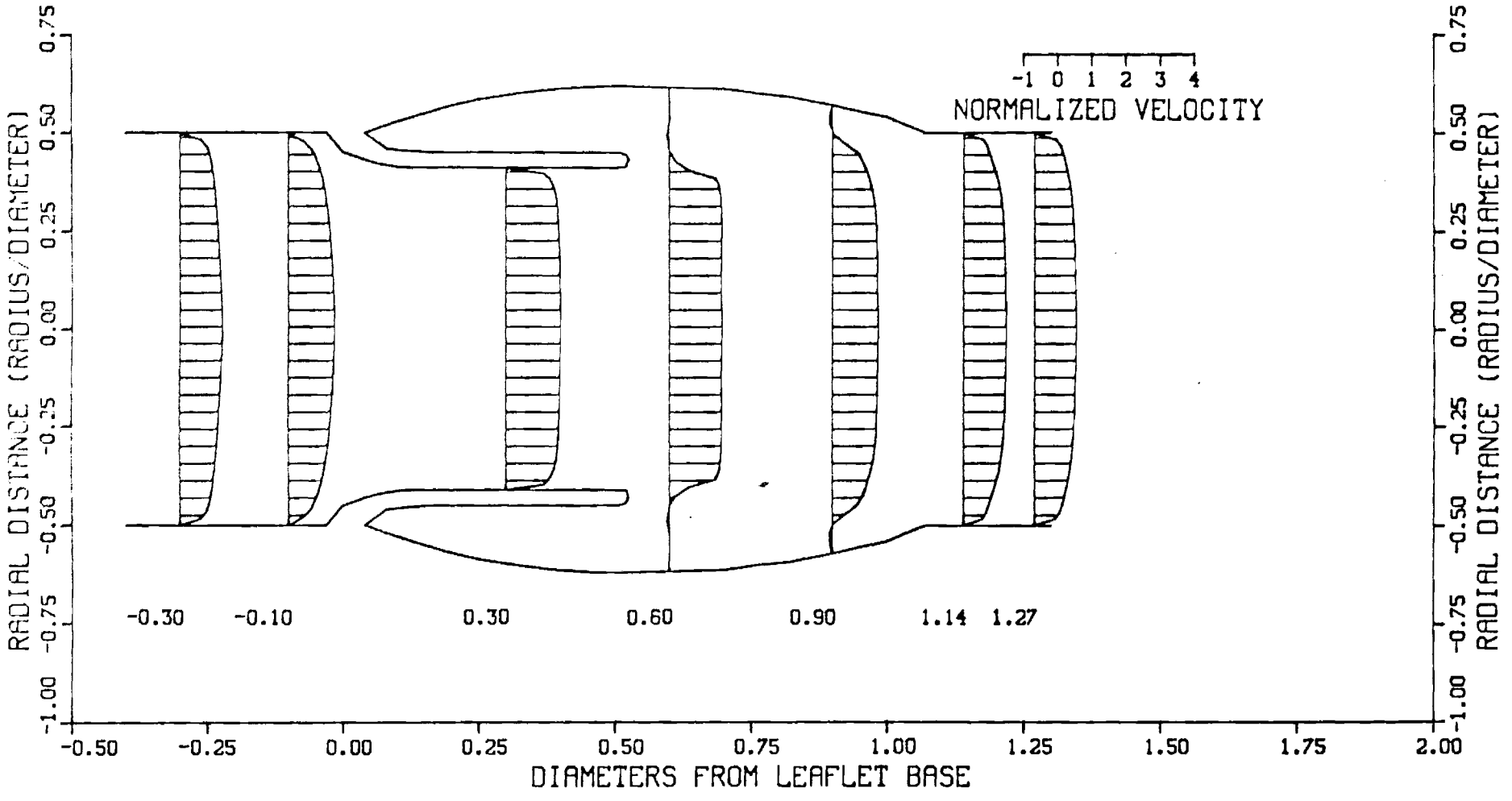

Figure 11: Velocity Profiles at Various Locations in Model A4

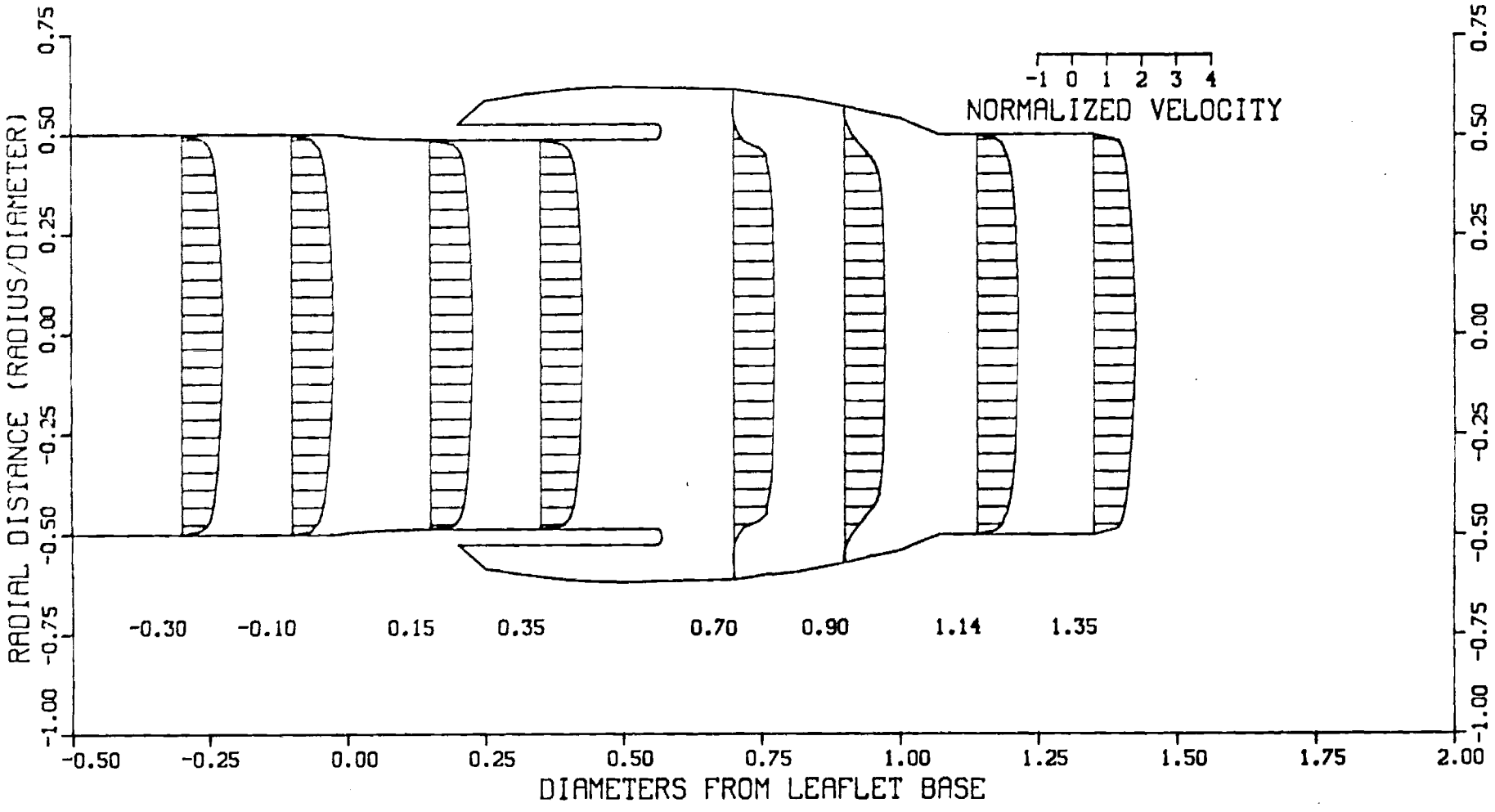

Figure 12: Velocity Profiles at Various Locations in Model A5

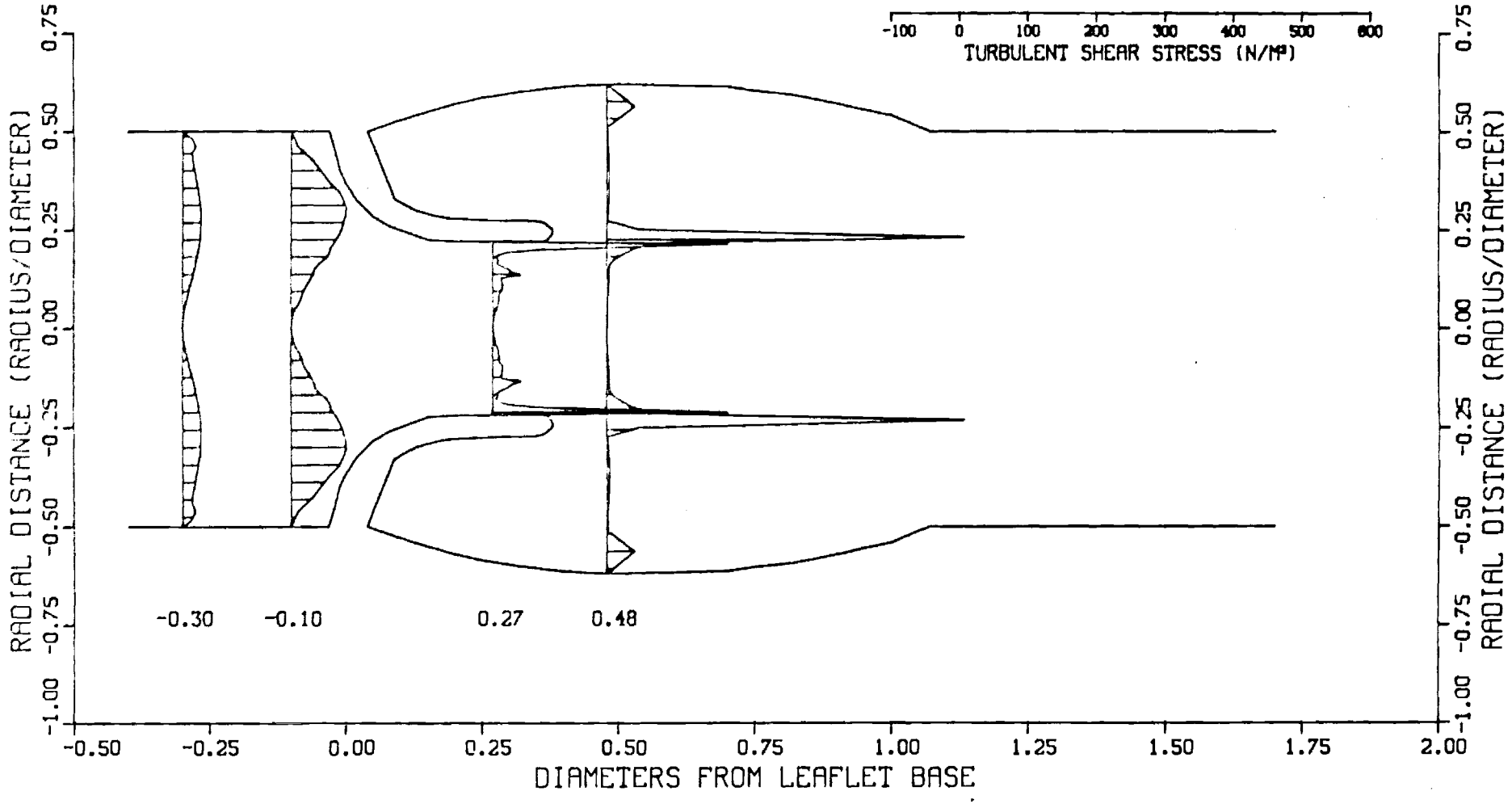

Figure 13: Turbulent Shear Stress Profiles at Various Locations in Model A1

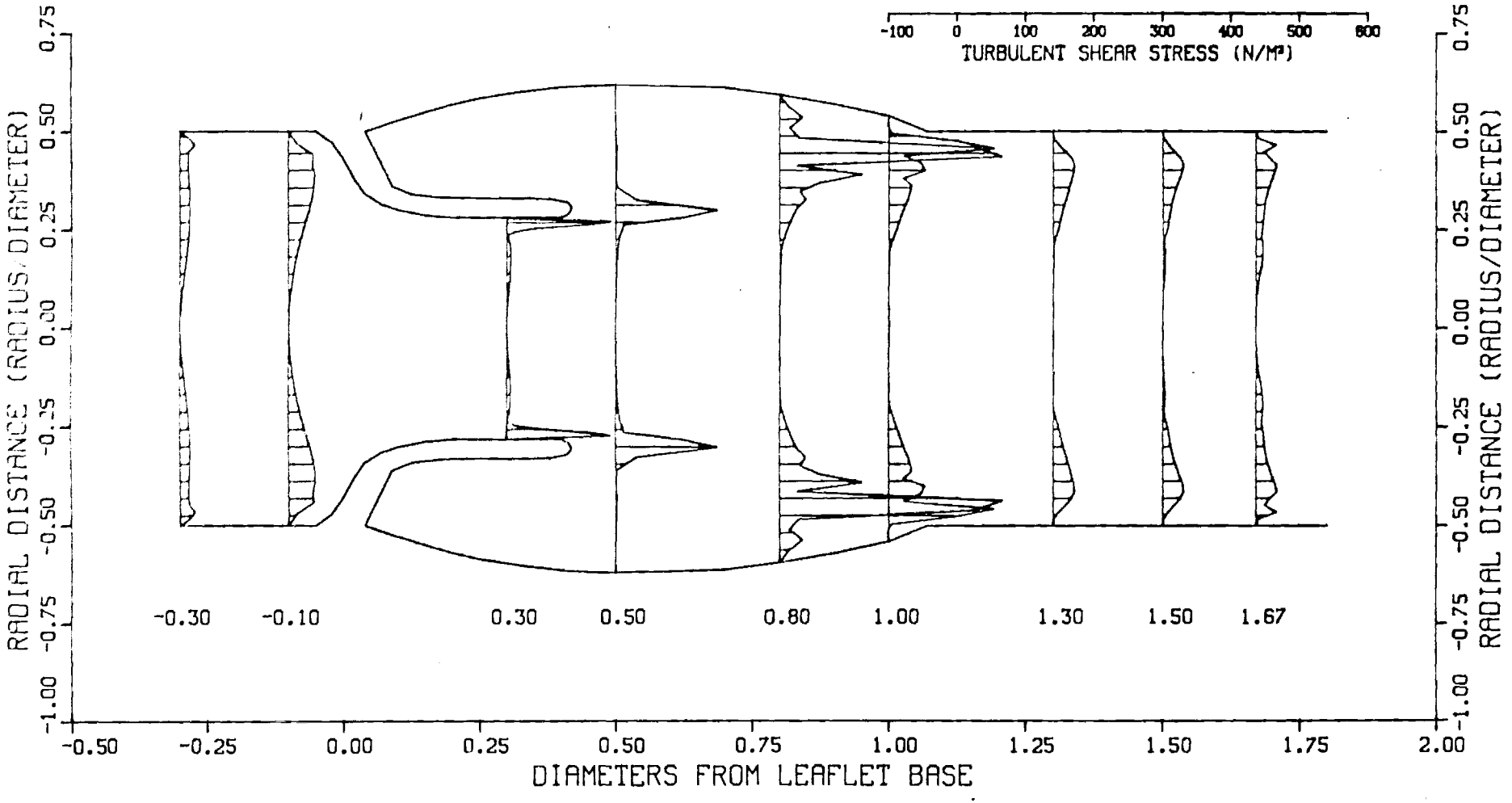

Figure 14: Turbulent Shear Stress Profiles at Various Locations in Model A2

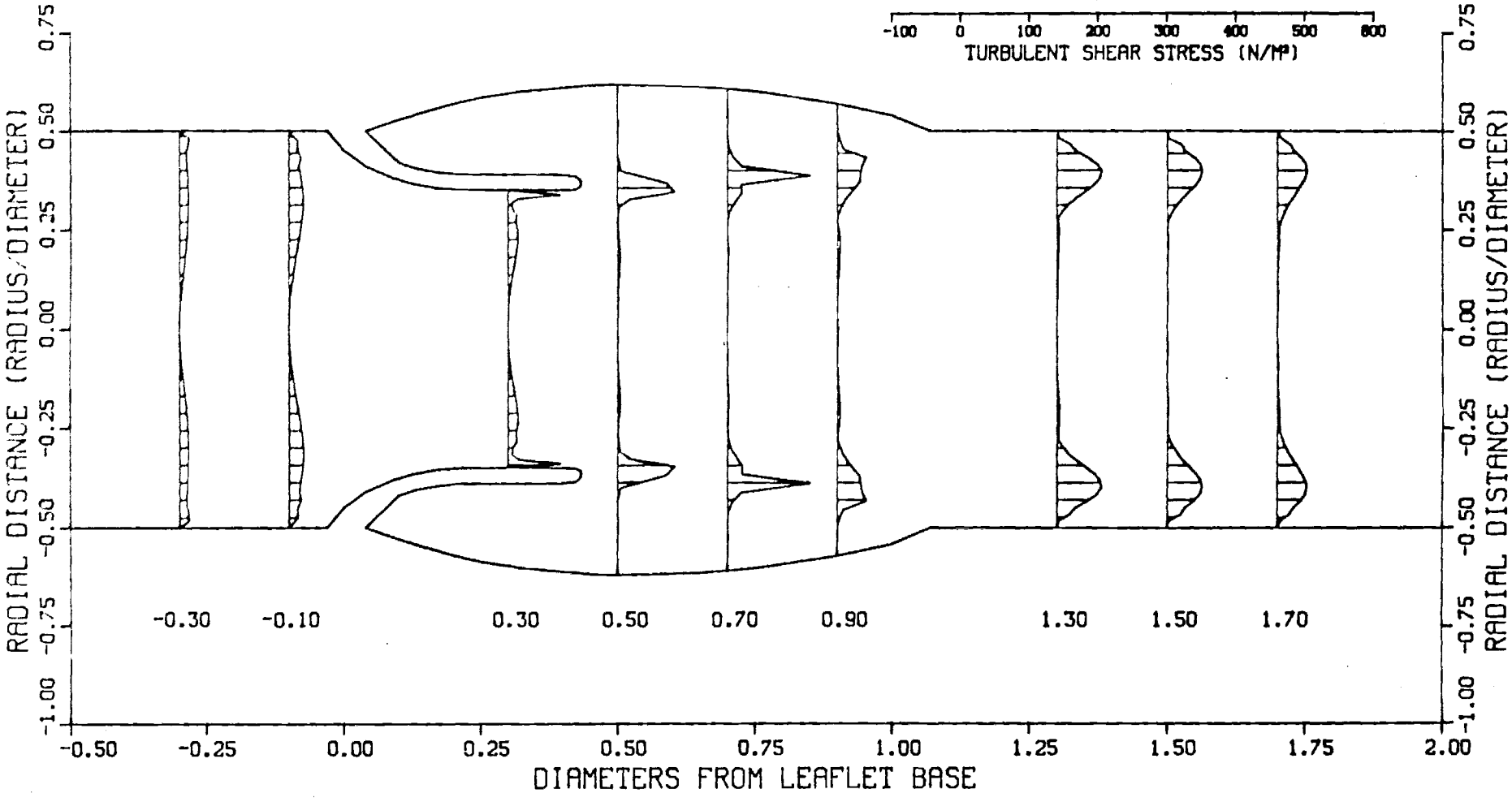

Figure 15: Turbulent Shear Stress Profiles at Various Locations in Model A3

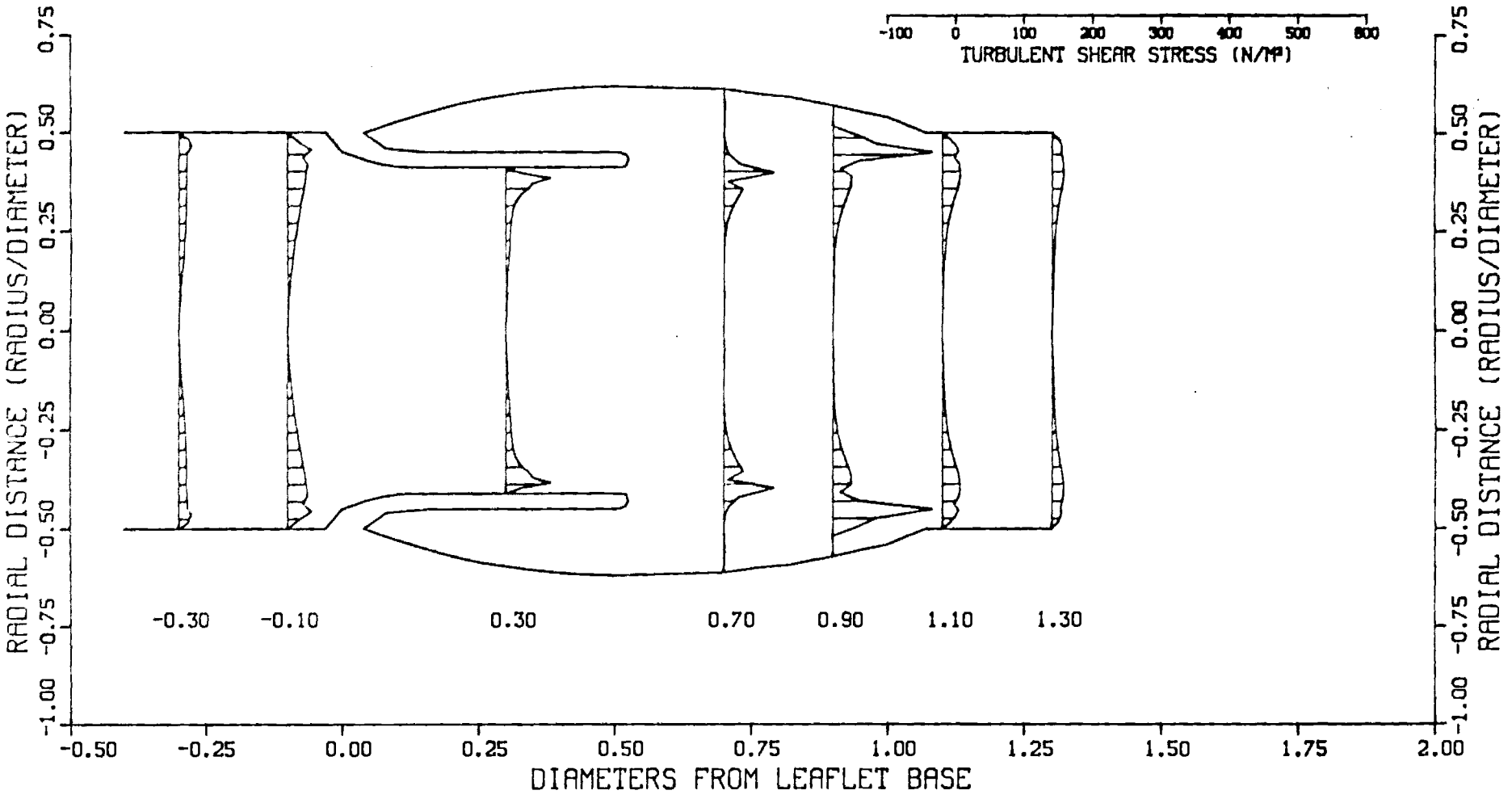

Figure 16: Turbulent Shear Stress Profiles at Various Locations in Model A4

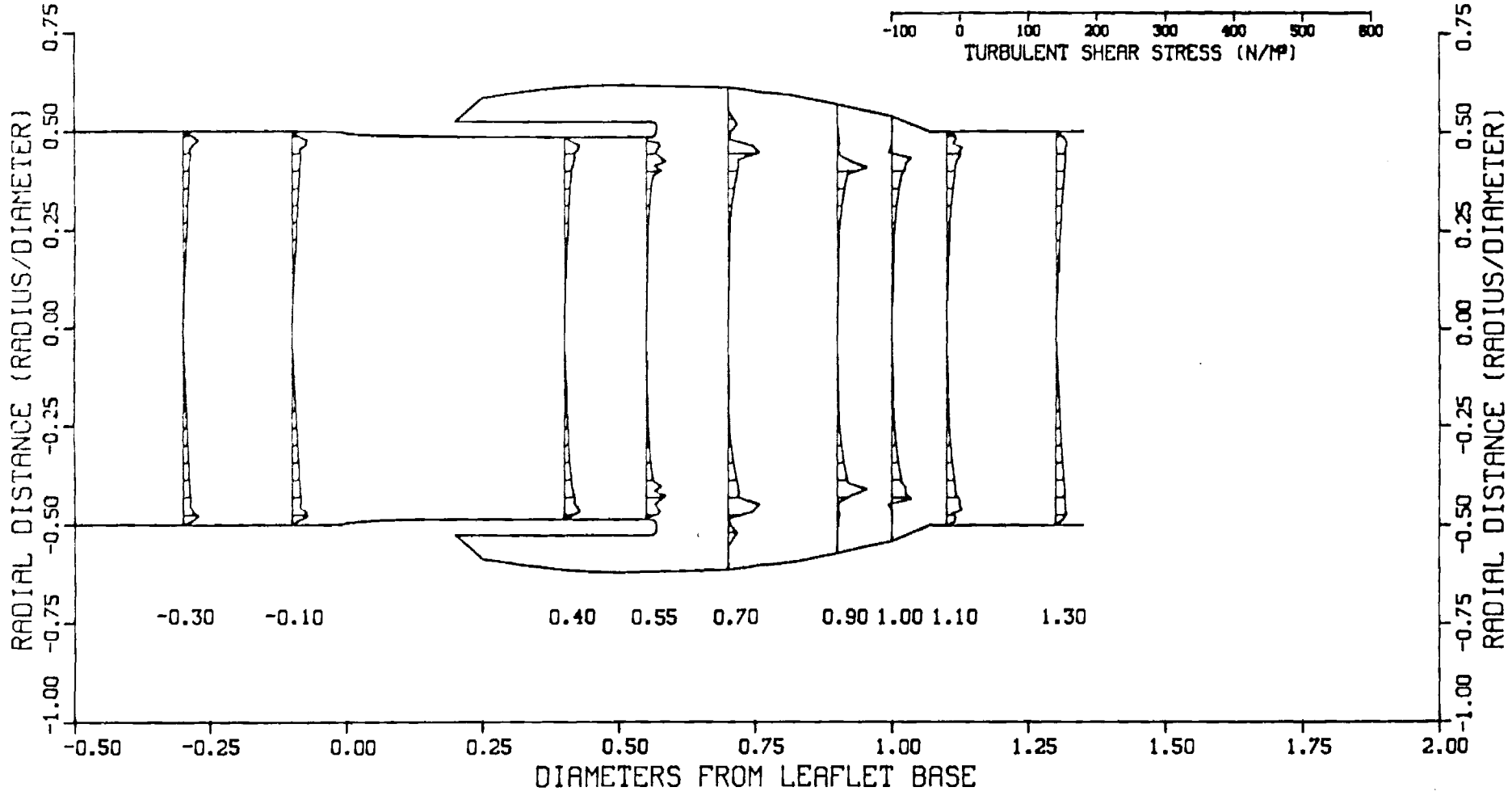

Figure 17: Turbulent Shear Stress Profiles at Various Locations in Model A5